ASIAN JOURNAL OF CHEMISTRY

Magnetic Characterization of Ca-Hexaferrites Using Hysteresis Technique

C.L. Khobaragade[1], S.V. Soni[2,*], A.K. Akant[3], R.K. Khatarkar[2], N.A. Wagdhare[1], C.B. Khobragade[1] and K.G. Rewatkar[4]

[1]Department of Applied Physics, Govindrao Wanjari College of Engineering & Technology, Nagpur-441 204, India
[2]Department of Applied Physics, Yeshwantrao Chavan College of Engineering, Nagpur-441 110, India
[3]Department of Physics, Manoharbhai Patel College of Engineering & Technology, Gondia-441 614, India
[4]Department of Physics, Dr. Ambedkar College, Deekshabhoomi, Nagpur-441 510, India

*Corresponding author: E-mail: s_sanjaysoni@rediffmail.com

In the present investigation the samples with chemical composition $Ca_{1-x-y}(CoTi)_{0.5}Mn_xZn_yFe_{11}O_{19}$ with (x = y = 0-0.5) were synthesized using perfect stoichiometric proportions of reacting oxides by standard ceramic technique. Hexagonal magnetoplumbite (M) structure having unit cell dimensions 'a' and 'c' which varies in the range between 5-6 Å and 21-23 Å with space group $P6_3/mmc$ (No. 194). The coercivity, retentivity, saturation magnetization and magnetic moment increases successively with increase in Mn-Zn concentration by changing magnetic field at 300 K. The room temperature resistivity increases in the range of 10^6 Ω cm. The grain size of the studied compounds varies in the range 0.29-0.79 mm (*i.e.*, 290-790 nm). The superexchange interaction, Me-O-Me is responsible for magnetic behaviour and found to increase with the increase of the Mn-Zn concentration in Ca-M compounds. It is found that there is a variation in hysteresis loops with change in magnetic field. The neutron diffraction and NMR studies also reveals that Co^{3+} ions are mainly distributed within $4f_{iv}$ and 12 k sites of the studied compound.

Key Words: Hexaferrite, Lattice parameters, Grain size, Magnetic parameters, Resistivity.

INTRODUCTION

The polycrystalline ferrites are low cost materials that have attractive microwave device applications owing to their high resistivity, mechanical strength, high transition temperature and high thermal stability. They can be easily synthesized by various techniques and do not require any special conditions for preparation. The Mn-Zn hexaferrites belong to the group of ferrite materials pertaining to high magnetic permeability and low loss. These materials are tailored to suit for microwave devices, computer memory chip, perpendicular magnetic recording, radio frequency coil, transformer coils and antennas *etc.*[1,2]. The intrinsic properties of Mn^{2+} and Zn^{2+} containing ferrites have been investigated[3,4], pertaining to high magnetic permeability and low loss.

In the present investigation, studies on coercivity, retentivity, saturation magnetization and magnetic moment measurements of the ferrites prepared by using low cost locally available Fe_2O_3 and added Mn-Zn as an impurity have been carried out. Investigations undertaken[5], highlight the behaviour of mixed ferrites with suitable addition of impurity. The studied material has high resistivity 10^6 Ω cm (Table-1) and has high density at room temperature. In the present work the different compositions (x = y = 0-0.5) of alloying metals (Mn and Zn) in the Ca-hexaferrites $Ca_{1-x-y}(CoTi)_{0.5}Mn_xZn_yFe_{11}O_{19}$ were incorporated.

TABLE-1
HYSTERESIS LOOP RESULTS OF $Ca_{1-x-y}(CoTi)_{0.5}Mn_xZn_yFe_{11}O_{19}$ COMPOUNDS

Compounds	Hc (Oe)	Br (Gauss)	σ_s (Gauss- cm^3/g)	η_B	Grain size (μm)
$Ca(CoTi)_{0.5}Fe_{11}O_{19}$	21.73	141.92	31.36	5.68	0.29
$Ca_{0.8}(CoTi)_{0.5}Mn_{0.1}Zn_{0.1}Fe_{11}O_{19}$	41.29	232.00	56.67	10.30	0.33
$Ca_{0.6}(CoTi)_{0.5}Mn_{0.2}Zn_{0.2}Fe_{11}O_{19}$	47.82	281.87	66.30	12.10	0.38
$Ca_{0.4}(CoTi)_{0.5}Mn_{0.3}Zn_{0.3}Fe_{11}O_{19}$	58.68	338.22	75.98	13.92	0.42
$Ca_{0.2}(CoTi)_{0.5}Mn_{0.4}Zn_{0.4}Fe_{11}O_{19}$	78.25	397.91	88.93	16.36	0.56
$(CoTi)_{0.5}Mn_{0.5}Zn_{0.5}Fe_{11}O_{19}$	93.46	480.17	101.47	18.75	0.79

Hc = Coercivity, Br = Retentivity, σ_s = Saturation magnetization, η_B = Magnetic moment.

EXPERIMENTAL

The synthesis of polycrystalline $Ca_{1-x-y}(CoTi)_{0.5}Mn_xZn_yFe_{11}O_{19}$ with (x = y = 0-0.5) samples were done by high temperature solid state diffusion reactions of stoichiometric mixtures of AR grade CaO, Fe_2O_3, TiO_2, MnO_2, CoO, ZnO oxides. The synthesis was divided into two steps: (i) after calcinations at 800 ºC for 2 h in air, the mixture was grinded and dried, compressed into pellets and (ii) finally subjected to a thermal treatment at 1040 ºC for 106 h with intermediate grinding and were quenched in air.

The XRD patterns were taken to identify the phases formed and to confirm the chemical reaction by using Phillips X-ray diffractometer using CuK_α-radiation with Ni as a filter. The X-ray diffraction pattern shows a single crystalline phase without traces of impurities. The patterns were indexed to hexagonal magnetoplumbite structure[6] belongs to the space group $P6_3/mmc$ (No. 194).

The coercivity, retentivity, saturation magnetization and magnetic moment were calculated from the hysteresis curve traced from CRO by applying changing magnetic field at room temperature. The grain size of the materials has been calculated from the scanning electron microscopic (SEM) study of the compounds.

RESULTS AND DISCUSSION

The hysteresis loop (Figs. 1-4) results of the compounds $Ca_{1-x-y}(CoTi)_{0.5}Mn_xZn_yFe_{11}O_{19}$ with (x = y = 0-0.5) were carried out as depicted in Table-1. The coercivity, retentivity, saturation magnetization and magnetic moment increases successively with increase of Mn-Zn concentration and decrease the concentration of non-magnetic compound. Because of ferrimagnetic (Mn-Zn), ferromagnetic (Fe) and non-magnetic (Ca) contents present in the formula unit.
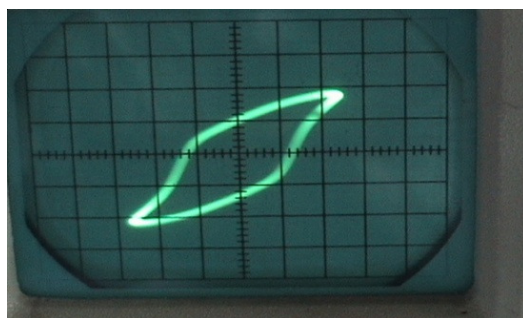
Fig. 1. B-H curve of compound $Ca(CoTi)_{0.5}Fe_{11}O_{19}$
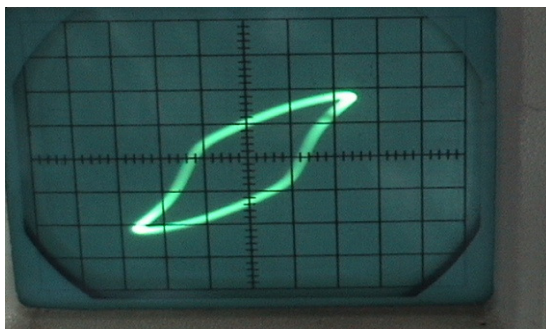
Fig. 2. B-H curve of $Ca_{0.8}(CoTi)_{0.5}Mn_{0.1}Zn_{0.1}Fe_{11}O_{19}$
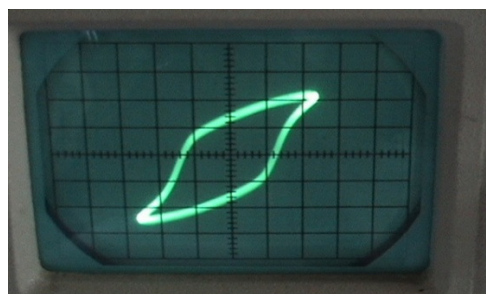
Fig. 3. B-H curve of $Ca_{0.6}(CoTi)_{0.5}Mn_{0.2}Zn_{0.2}Fe_{11}O_{19}$
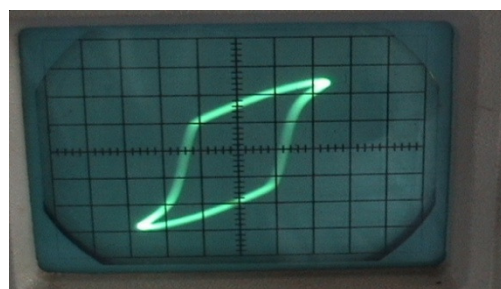
Fig. 4. B-H curve of $Ca_{0.4}(CoTi)_{0.5}Mn_{0.3}Zn_{0.3}Fe_{11}O_{19}$

Successive increase in the value of saturation magnetization is due to the substitution of Mn-Zn in the spinel blocks of the M-structure occupying the octahedral sites (12k). The interaction energy increase high which in turn increases the saturation magnetization[7]. Also this increase of saturation magnetization is due to the presence of Fe^{3+} and Mn^{2+}-Zn^{2+} ions, which have high magnitude superexchange interactions, particularly when all the 24 sites (2a, 2b, 4f1, 4f2 and 12k) are filled by magnetic and ferromagnetic ions. The 2a-12k interaction is stronger as compare to 2a-4f1 and 4f1-12k interactions. 2a-12k interaction particularly takes part to increase the magnetic characterization[8].

Typical grains of compounds $Ca_{1-x-y}(CoTi)_{0.5}Mn_xZn_yFe_{11}O_{19}$ with (x = y = 0-0.5) were calculated, which are in the range of 0.29-0.79 mm (*i.e.*, 290-790 nm) (Table-1). A microscopic observation at room temperature showed that the grains attracted by a magnet and their [001] directions were oriented parallel to the lines of magnetic force. Hence the increase in saturation magnetization depends on grain size.

Coercivity (Hc) carried out from the plot between loop width (in mm) or $2e_x$ and applied magnetic field (Fig. 5) for various compounds from the hysteresis loop *i.e.*, from B-H curve. From this curve it is observed that coercivity continuously increases with the increase of Mn-Zn concentration for increasing magnetic field at room temperature (300 K).

Retentivity (Br) calculated from the plot between 2 x intercept (in mV) or 2(ey)r on y-axis and applied magnetic field (Fig. 6) for different compounds. It shows increasing trend along y-axis from hysteresis loops *i.e.*, retentivity (residual magnetism) increases with increase in Mn-Zn concentration at room temperature.

Saturation magnetization (ss) calculated from the plot between tip to tip height (in mV) or 2(ey)s and applied magnetic field (Fig. 7) from hysteresis loops for different compounds. It shows increase in saturation magnetization with increase in Mn-Zn concentration for increase in magnetic field at room temperature. All these three parameters calculated from the B-H curve which is shown in above (Figs. 1-4).
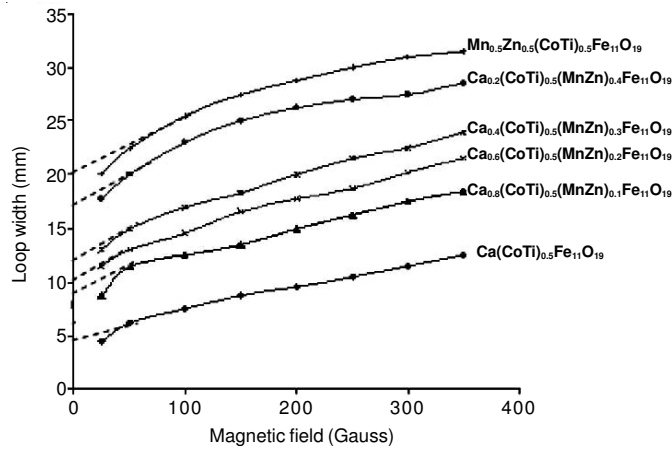
Fig. 5. Plot of loop width *versus* applied magnetic field of compounds $Ca_{1-x-y}(CoTi)_{0.5}Mn_xZn_yFe_{11}O_{19}$ with (x = y = 0-0.5)
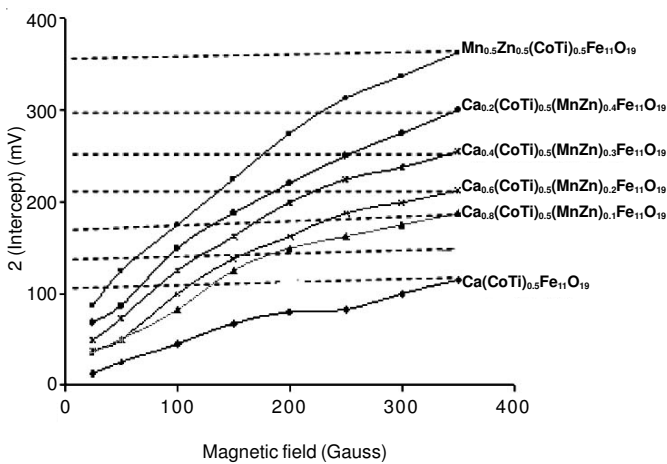
Fig. 6. Plot of 2 x Intercept (in mV) *versus* applied magnetic field of compounds $Ca_{1-x-y}(CoTi)_{0.5}Mn_xZn_yFe_{11}O_{19}$ with (x = y = 0-0.5)
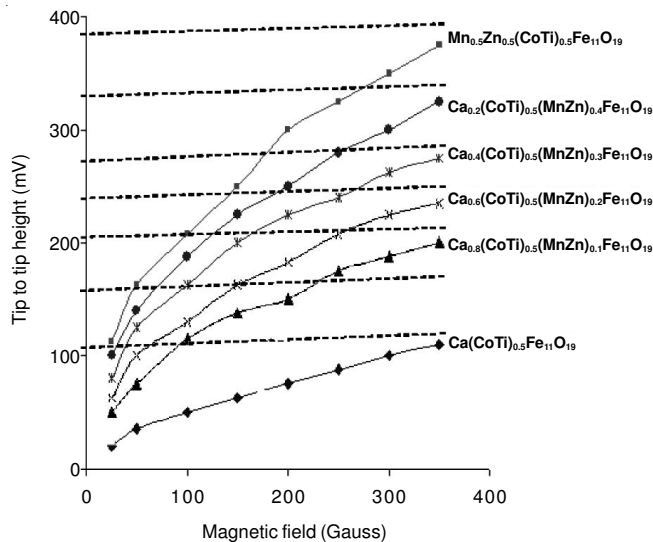
Fig. 7. Plot of tip to tip height (in mV) *versus* applied magnetic field of compounds $Ca_{1-x-y}(CoTi)_{0.5}Mn_xZn_yFe_{11}O_{19}$ with (x = y = 0-0.5)

The magnetic moment (η_B) calculated from the equation

$$\eta_B = \frac{M \times Ms}{5585 \times d}$$

$$= \frac{M \times \sigma_s}{5585} \text{ (since MS/d = } \sigma_s)$$

where M, molecular weight of compound, σ_s, saturation magnetization (Gauss cm^3/g), d, mass (bulk) density and Ms, saturation magnetization (Gauss). Magnetic moments increases with increase of Mn-Zn concentration at room temperature because of Ti^{4+} ions are distributed within $4f_2$ and 12k sites[9], Co^{2+} ions occupy $4f_1$ and 12k sites[10]. Hence due to $4f_1$ and $4f_2$ with down spin have large value of magnetic moment can be obtained according to cationic distribution deduced from the neutron and NMR studies.

The 12k sublattice (spin up) is antiferromagnetically coupled with the 2b (spin up) and 2a as well as the 12k inter-sublattice interactions and have only perturbing effect on the orientation of magnetic moment of 12k ions (Table-2). The neutron diffraction and NMR studies also reveals that Co^{3+} ions are mainly distributed within $4f_{iv}$ and 12k sites[11,12].

TABLE-2
STRUCTURAL AND MAGNETIC CHARACTERIZATION
OF THE MAGNETIC SUBLATTICE IN THE
MAGNETOPLUMBITE STRUCTURE

Sub-lattice	Co-ordination	Block	No. of ions (FU)	Spin direction
2a	Octahedral	S	1	Up
2b	Pseudo-tetrahedral	R	1	Up
$4f_1$	Tetrahedral	S	2	Down
$4f_2$	Octahedral	R	2	Down
12K	Octahedral	S-R	6	Up

The measurements of coercivity (Hc), retentivity (Br), saturation magnetization (σ_s) and magnetic moment (η_B) imply an increase with Fe^{3+} and Mn^{2+}-Zn^{2+} ion concentration in series, which are indication of ferromagnetic nature of the compounds. The continuous increase in Hc, Br, σ_s and η_B with increase of Mn and Zn contents may be explained by assuming that Mn^{2+}, Zn^{2+} substitution is preferentially performed on the spin up magnetic sublattice for the composition.

The strong increase in Hc, Br, σ_s and η_B demonstrates that some inter sublattice exchange interactions are dominant. It can be seen that the spin co-linearity appears mostly in the spin up sublattice, especially the 12k sublattice has degree of frustration being in this way strongly affected by increase of 12k-$4f_{iv}$ interaction. A mean field analysis of the exchange interaction in BaM hexaferrites has been carried out[13]. The results shows that the Fe (12k) sublattice making a link among R and S structural block is subjected to very strong competitive exchange interactions (Table-2). So, when the Fe^{3+} ions in the 12k sublattice are substituted by ferromagnetic ions, strongest nature of the superexchange interaction between magnetic ions results in a fairly inclined ferrimagnetism. The shape of the hysteresis loop depends on the domain state of the grains in the sample[14].

In case of M-structure predominant superexchange inter-action is due to 1-oxygen-2 ions in which appertaining angle f is large (*ca.* 140º), whereas the other interaction, the 2-oxygen-3 interaction which attempt to align the magnetic moments of these ions antiparallel, is smaller because the appertaining angle is unfavourable (*ca.* 80º). The change in

saturation magnetization values with different substitutions replacing calcium can be explained on the basis of the gravity and nature of particular interactions involved in the lattice.

There are at least three causes for the deviation of magnetic moment: (i) The ions distribution may not be the same. (ii) The ions may have in additions to a spin moment and orbital moment (iii) The deviation in bond angle arise due to localized distortions keeping bulk symmetry unaffected[15].

The values of coercivity and retentivity may differ slightly because they also depend on the grain size[16]. In M-type compounds, the orientations of the magnetic moments of the ferric ions in the crystals are generally aligned along the c-axis in antiparallel with each other. This alignment occurs due to the superexchange interaction through oxygen ions which is responsible for spin alignment[17,18].

Conclusion

As Mn-Zn concentration increases coercivity, retentivity, saturation magnetization and magnetic moment increase successively. So that we found that there is a variation in hysteresis loops with change in magnetic field. These magnetic parameters also depended on the grain size of the materials which varies in the range of 0.29-0.79 μm (*i.e.*, 290-790 nm). The superexchange interaction, Me-O-Me is responsible for magnetic behavoiur and found to increase with the increase in the Mn-Zn concentration in Ca-M compounds.

REFERENCES

1. J. Lipka, A. Gruskova, O. Orlicky, J. Sitek, M. Miglierini, R. Grone, H. Huel and M. Toth, *Hyperfine Interactions*, **59**, 381 (1990).

2. R. Muller, H. Pfeiffer and W. Schuppel, *J. Magn. Mater.*, **18**, 101 (1991).

3. K.C. Han, H.D. Choi, T.J. Moon, W.S. Kim and K.Y. Kim, *J. Mater. Sci.*, **30**, 3567 (1995).

4. S.R. Murthy, *Bull. Mater. Sci.*, **26**, 499 (2003).

5. C. Heck, Editor, Magnetic Materials and Their Applications, Butterworth Co. Ltd. London (1974).

6. M.E. De Roy, J.P. Besse, R. Chevalier and M.G. Gasperin, *J. Solid State Chem.*, **67**, 185 (1987).

7. X. Obrador, A. Isalgue, A. Colomb, M. Pernet, J. Pernet, J. Rodriguez, J. Teheda and J.C. Jouberg, *IEEE Trans, Magn.*, **20**, 1636 (1984).

8. H. Stepankowa, J. Kohout and Z. Simsa, Proc. ICM., Amsterdam: North Holland, Vol. 3, p. 705 (1991).

9. B.X. Gu, H.Y. Zang, H.R. Zhai, B.G. Shen, M. Lu, S.Y. Zhang and Y.Z. Maoi, *Phys. Start Sol. (a)*, **133**, K83 (1992).

10. L. Kelvoda, Dlonha and M. Vratislov, *J. Magn. Magn. Mater.*, **87**, 243 (1990).

11. N.F.M. Henry, H. Lipson and W.A. Wooster, The Interpretation of X-Ray Diffraction Photographs, London: McMillan & Co. (1953).

12. J. Smit and H.P.J. Wijn, Ferrites, Philips Technical Library, Eindhoven, pp. 177-210 (1959).

13. A. Isalgue, A. Labarta, J. Tejada and X. Obradors, *Appl. Phys. A*, **39**, 221 (1986).

14. A.M. Sankpal, S.S. Suryawansh, S.V. Kakatkat, G.G. Tengshe, R.S. Patil, N.D. Chaudhari and S.R. Sawant, *J. Magn. Magn. Mater.*, **186**, 349 (1998).

15. J. Smit and H.P.J. Wijn, Ferrites, Philips Technical Library, Eindhoven, The Netherlands (1959).

16. A. van der Lee, M. Evain, M. Mansuetto, L. Monconduit, R. Brec and J. Rouxel, *J. Solid State Chem.*, **111**, 75 (1994).

17. L. Neel, Magnetic Properties of Ferrites; Ferrimagnetism and Antiferromagnetism, (in Fr.) Ann. Phys. (Paris), pp. 3137-98 (1948).

18. P.W. Anderson, *Phys. Rev.*, **79**, 350 (1950.